ARTICLE NO. 79-0722R

C80-078

Divergence of Forward Swept Composite Wings

80001
80003
80004

Terrence A. Weisshaar*
Virginia Polytechnic Institute and State University, Blacksburg, Va.

Forward swept wing aircraft may have superior aerodynamic performance for certain missions. Algebraic expressions to predict the static aeroelastic divergence characteristics of forward swept wings constructed of composite materials have been developed using a laminated box beam model to describe the wing structure and aerodynamic strip theory to predict the loads due to wing bending and torsional deformation. The expressions presented show that, because of elastic coupling between wing bending and torsion, wing divergence may be precluded for reasonably large forward sweep angles if the composite structure is properly tailored. The structural parameters that maximize divergence speed are readily identified. Two illustrative examples are presented.

Nomenclature

a_o = two-dimensional lift curve slope
b = box chord length, measured perpendicular to the reference axis
e = distance between wing quarter-chord and reference axis, positive aft
f = $1-\eta(1-\lambda)$
g = composite torsional coupling parameter, K/GJ
$h(y)$ = bending deflection of the reference axis of the wing, positive upward
k = nondimensional bending coupling parameter, K/EI
l = wing semispan dimension, measured along the reference axis
q = dynamic pressure, $\frac{1}{2}\rho V^2$
w = h/l
y = distance along reference axis, measured from wing root
$\alpha(y)$ = torsional deformation of wing sections about the reference axis, positive nose-up
α_e = $\alpha-\Gamma \tan \Lambda$
Γ = dh/dy
η = y/l
θ = fiber angle with respect to a rearward normal to the reference axis
λ = taper ratio = c_{tip}/c_{root}
Λ = sweep angle of the reference axis, positive for sweepback

Introduction

THE expanding development of modern laminated composite materials for aircraft structural components has led engineers to seek new ways to exploit further the directional strength and stiffness properties of these lightweight materials. One facet of this search has been the study of the potential for enhancing the aeroelastic performance of an airfoil through aeroelastic tailoring of the support structure. Aeroelastic tailoring of a lifting surface involves the synthesis of a composite structure whose special directional properties elastically couple the basic structural deformations, such as bending and torsion, in an advantageous manner. The purpose of this paper is to illustrate an application of the aeroelastic tailoring concept to swept wings; specifically, this application involves the design of composite material wing skins to enhance static aeroelastic divergence characteristics of forward swept wings.

The first aircraft to employ a forward swept wing was the Junkers JU 287 four-engine jet bomber,[1] developed as a test aircraft in Germany during World War II. This test aircraft flew on 16 occasions in 1944, developing speeds of over 650 km/h (404 mph). The wing of the Ju 287 was swept forward approximately 25 deg, primarily for the purpose of providing good low-speed flight characteristics. Limited flight tests did not disclose any severe aeroelastic or directional stability problems.

Studies after World War II[2,3] disclosed that low static aeroelastic divergence speeds were associated with swept forward wings unless they were stiffened significantly. Ref. 3 shows convincingly that, from a static aeroelastic stability point of view, sweptback metallic wings are far superior to forward swept metallic wings. Because of this fact, the forward swept metallic wing has not been a serious design concept for some time, although a proposed bomber, the Convair B-53, was to use forward swept wings[4] and the modern day HFB 320 Hansa twin jet executive transport uses a forward swept wing.[5] The metallic wing on the HFB 320 employs 15 deg of forward sweep at the quarter-chord line to avoid running the main spar of the wing through the passenger cabin.

From a design optimization standpoint, interest in swept wings has been confined to sweptback configurations. However, as early as 1931, Knight and Noyes[6] noted that wings with 20 deg of forward sweep experience stall at higher angles of attack than similar 20 deg sweptback wings. Thus, forward swept wings may develop higher lift coefficients than sweptback wings. It is known also that rearward sweep may produce a pronounced rolling or pitching instability at high angles of attack because of premature tip stall. Conversely, at high angles of attack, forward swept wings begin to stall first at the wing root and thus are not susceptible to these instabilities. In fact, recent unpublished research indicates that forward swept wing aircraft may be highly spin resistant at high angles of attack.

Renewed interest in forward swept wing technology is due to Krone[7]. Krone discusses the feasibility of the forward swept wing concept when laminated composite materials, rather than metals, are used for the wing skin. His conclusion, arrived at through a comprehensive set of numerical examples, is that laminated composites provide the design

Presented as Paper 79-0722 at the AIAA/ASME/ASCE/AHS 20th Structures, Structural Dynamics, & Materials Conference, St. Louis, Mo., April 4-6, 1979; submitted May 7, 1979; revision received Nov. 7, 1979.

Index categories: Aeroelasticity and Hydroelasticity; Structural Composite Materials; Structural Design.

*Associate Professor, Aerospace and Ocean Engineering Dept. Member AIAA.

flexibility to overcome the severe weight penalties encountered in conventional metallic forward swept wing design.

The results of Ref. 7 leave unsettled several questions about the mechanism by which static aeroelastic stability improvements may be achieved through the use of laminated composites. The present paper seeks to provide a basic understanding of this phenomenon. Attention in the discussion to follow is focused upon the elastic coupling between wing bending and torsional deformations introduced by laminated composite construction, and the influence of this coupling upon divergence of moderate to high aspect ratio swept wings.

To accomplish these objectives, the present study employs laminated beam theory to represent the wing structure and uses aerodynamic strip theory to compute the loads that arise from wing deformation. This method of formulation allows an analytical solution from which the importance of geometrical, structural, and aerodynamic parameters can be discerned.

Analytical Model

The structural idealization of the high aspect ratio wing used in this study is similar to that employed by Housner and Stein[8] to study the flutter of sweptback laminated composite wings. The model used in Ref. 8 is valid only for balanced ply, symmetrical laminates. An alternative, but similar, development of a coupled bending-torsion composite wing model is described in Ref. 9, but was not used in this analysis.

The bending and torsional stiffnesses of the wing are assumed to arise solely from thin, laminated composite cover-sheets forming the upper and lower surfaces of the wing. The equivalent bending and torsional stiffnesses of the resulting box beam are computed by using classical Euler-Bernoulli beam deformation assumptions. With these assumptions, the deformation of a chordwise section of the wing, perpendicular to the straight reference axis shown in Fig. 1, is assumed to be due to three distinct types of deformation: a bending deflection $h(y)$, positive upward; a rotation $\alpha(y)$, positive nose-up; and a stretching displacement $v_o(y)$ along the y axis. All deflections are measured with respect to an undeformed y axis, lying in the geometrical mid-plane of the wing box, midway between the upper and lower surfaces and equidistant between the front edge and the rear edge of the structural box. The beam model also assumes an effective root and tip to be located as shown in Fig. 1.

Each individual lamina of the cover-sheet laminates is itself orthotropic with respect to a set of principal axes, one principal axis being oriented in the lamina fiber direction, while the other axis is perpendicular to these fibers. These principal axes, denoted as axis 1 and axis 2 in Fig. 2, lie in a plane parallel to the x-y reference plane of the wing and are oriented at an angle θ to the x-y system, measured positive as shown in Fig. 2.

For a typical lamina, the relationship between inplane stresses and strains, measured in the x,y reference system, may be expressed in matrix form as[10].

$$\begin{Bmatrix} \sigma_{xx} \\ \sigma_{yy} \\ \tau_{xy} \end{Bmatrix} = \begin{bmatrix} \bar{Q}_{11} & \bar{Q}_{12} & \bar{Q}_{16} \\ \bar{Q}_{12} & \bar{Q}_{22} & \bar{Q}_{26} \\ \bar{Q}_{16} & \bar{Q}_{26} & \bar{Q}_{66} \end{bmatrix} \begin{Bmatrix} \epsilon_{xx} \\ \epsilon_{yy} \\ \gamma_{xy} \end{Bmatrix} \tag{1}$$

The terms $\bar{Q}_{ij}$ are functions of the angle θ and the orthotropic elastic moduli of the lamina. These terms are derived and defined in Ref. 10.

The formulation of the equations of equilibrium that govern the divergence problem is best approached via strain energy methods. The N laminae comprising the upper and lower surfaces of the wing box are constrained to act as a unit in a manner prescribed by the Euler-Bernoulli deformation assumptions. The total strain energy of the wing box, denoted as U, is written as follows (note that $(\,)' = \mathrm{d}(\,)/\mathrm{d}y$):

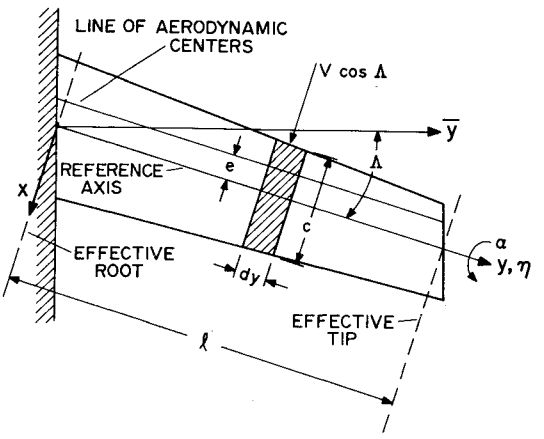

Fig. 1 Slender swept wing geometry with typical chordwise segment illustrated.

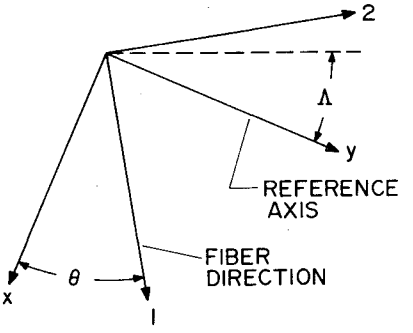

Fig. 2 Lamina principal axis orientation with respect to wing reference axes.

$$U = \int_o^l \{ \tfrac{1}{2} EI_o (h'')^2 - K_o (h'' \alpha') + \tfrac{1}{2} A_{22} (v_o')^2 + B_{33} (v_o' \alpha') - B_{22} (h'' v_o') + \tfrac{1}{2} GJ_o (\alpha')^2 \} \mathrm{d}y \tag{2}$$

The terms multiplying the deflection derivatives in Eq. (2) are defined as follows:

$$EI_o = \bar{b} \left[\sum_{i=1}^{N} \bar{Q}_{22}^{(i)} \beta_i \right] \tag{3a}$$

$$GJ_o = \bar{b} \left[\sum_{i=1}^{N} 4 \bar{Q}_{66}^{(i)} \beta_i \right] \tag{3b}$$

$$K_o = \bar{b} \left[\sum_{i=1}^{N} 2 \bar{Q}_{26}^{(i)} \beta_i \right] \tag{3c}$$

$$A_{22} = \bar{b} \left[\sum_{i=1}^{N} \bar{Q}_{22}^{(i)} t_i \right] \tag{3d}$$

$$B_{22} = \bar{b} \left[\sum_{i=1}^{N} \bar{Q}_{22}^{(i)} \delta_i \right] \tag{3e}$$

$$B_{33} = 2\bar{b} \left[\sum_{i=1}^{N} \bar{Q}_{26}^{(i)} \delta_i \right] \tag{3f}$$

The summation used in Eqs. (3) extends over the N layers of composite material. The constants β_i and δ_i are defined in terms of a lamina coordinate z measured positive upward

from the box middle surface. In terms of the lamina thickness t_i and lamina lower and upper position coordinates z_i and z_{i+1}, respectively, β_i and δ_i are defined as follows

$$\beta_i = \int_{z_i}^{z_{i+1}} z^2 dz = \frac{1}{3}(t_i^3 + 3t_i z_i^2 + 3z_i t_i^2) \tag{4}$$

and

$$\delta_i = \int_{z_i}^{z_{i+1}} z dz = t_i(z_{i+1} + z_i)/2 \tag{5}$$

The term β_i represents the area moment of inertia of a strip of material, of thickness t_i and unit width, about the middle surface. As such, β_i is always a positive number. Term δ_i represents the first moment of the area of the same strip about the middle surface. This term δ_i is positive if the lamina area centroid lies above the middle surface and negative if it does not.

Equation (2) indicates that the bending deformation $h(y)$ is elastically coupled both to the torsional deformation $\alpha(y)$ and to the extensional deformation of the middle surface $v_o(v)$. This extensional deformation will be zero if the middle surface is the neutral surface for bending, a situation that occurs only when the upper and lower cover-sheets are geometrically and elastically symmetrical about the middle surface.

The Principal of Virtual Work can be used to derive the differential equations governing static equilibrium of the laminated beam under the action of an upward distributed load $p(y)$ and a distributed torque $t(y)$. These equations, derived in Ref. 11, are found to be

$$[EIh'' - K\alpha]'' = p(y) \tag{6}$$

$$[-Kh'' + GJ\alpha']' = -t(y) \tag{7}$$

Note that, in Eqs. (6) and (7), $(\ )' = d(\ )/dy$.

The terms EI, GJ, and K are defined, in terms of the parameters appearing in the strain energy expression and defined in Eqs. (3) as:

$$EI = EI_o - (B_{22})^2/A_{22} \tag{8a}$$

$$GJ = GJ_o - (B_{33})^2/A_{22} \tag{8b}$$

$$K = K_o - B_{22}B_{33}/A_{22} \tag{8c}$$

Equations (6) and (7) result when the v_o degree of freedom is eliminated because the resultant axial force, internal to the beam, is zero. Thus, v_o can be expressed as a function of derivatives of $h(y)$ and $\alpha(y)$.

The parameter K provides elastic coupling between bending and torsion not present in conventional metallic beam analysis. This parameter is seen to be both a function of the laminate stacking sequence and the lamina fiber orientation angles. Therefore, an opportunity to tailor the wing structure for optimal bending-torsion coupling is presented.

The boundary conditions for a cantilevered wing consist of the usual displacement and slope conditions at the wing root:

$$\alpha(0) = h(0) = \frac{dh}{dy}(0) = 0 \tag{9}$$

The resultant bending moment, shear force, and torque conditions at the wing tip are written as:

$$M(l) = EIh'' - K\alpha' = 0 \tag{10a}$$

$$V(l) = [EIh'' - K\alpha']' = 0 \tag{10b}$$

$$T(l) = GJ\alpha' - Kh'' = 0 \tag{10c}$$

To complete the governing equations for the divergence problem, the only aerodynamic loads considered are those due to bending deformation $h(y)$ and torsional deformation $\alpha(y)$. Taking chordwise wing sections as illustrated in Fig. 1, the lift force per unit length, positive upward, is

$$p(y) = qca_o\cos^2\Lambda(\alpha - \frac{dh}{dy}\tan\Lambda) \tag{11}$$

while the torque per unit length is

$$t(y) = qcea_o\cos^2\Lambda(\alpha - \frac{dh}{dy}\tan\Lambda) \tag{12}$$

The term a_o appearing in Eq. (11) and (12) is the two-dimensional lift curve slope of the chordwise sections and may be empirically corrected to reflect the effects of finite wing span, sweep, and compressibility.

The behavior of two types of wing planforms will be presented: 1) untapered, uniform property, swept wings; and 2) swept wings with linear taper and geometrically similar cross sections.

Attention will first turn to the solution of the previously discussed equations to determine the divergence speed of an untapered swept wing constructed of laminated composites.

Divergence of Swept Wings with Untapered Planforms

The governing equations for static aeroelastic divergence of a swept composite wing, of the type described previously, may be written in nondimensional form as follows:

$$\Gamma''' - k\alpha''' = a(\alpha - \Gamma\tan\Lambda) \tag{13}$$

$$\alpha'' - g\Gamma'' = -b(\alpha - \Gamma\tan\Lambda) \tag{14}$$

where $(\ )'$ now represents $d(\ )/d\eta$. The nondimensional parameters in Eqs. (13) and (14) are:

$$a = qcl^3a_o\cos^2\Lambda/EI \tag{15}$$

$$b = qcel^2a_o\cos^2\Lambda/GJ \tag{16}$$

The boundary conditions in Eqs. (9) and (10) can be transformed similarly into nondimensional form.

As in the case of the metallic wing discussed in Ref. 3, Eqs. (13) and (14) may be combined into a single equation by defining a new variable, denoted as α_e, and defined as

$$\alpha_e = \alpha - \Gamma\tan\Lambda \tag{17}$$

This new variable represents the angle of attack of a chordwise section of the wing induced by torsional and bending deformation of the wing.

Equations (13) and (14) can be combined to give the following third-order differential equation with constant coefficients,

$$\alpha_e''' + \left[\frac{b(1-k\tan\Lambda)}{(1-kg)}\right]\alpha_e' - \left[\frac{a(g-\tan\Lambda)}{(1-kg)}\right]\alpha_e = 0 \tag{18}$$

The boundary conditions associated with Eq. (18) are as follows:

$$\alpha_e(0) = 0 \tag{19}$$

$$\alpha_e''(1) = 0 \tag{20}$$

$$\alpha_e''(1)+\left[\frac{b(1-k\tan\Lambda)}{1-kg}\right]\alpha_e(1)=0 \tag{21}$$

When $k = g = 0$, Eq. (18) and its boundary conditions reduce to those developed in Ref. 3.

Two aeroelastic parameters appear in Eq. (18). These parameters are defined as

$$\bar{a}=\left[\frac{1-k\tan\Lambda}{1-kg}\right]\left[\frac{qcel^2a_o\cos^2\Lambda}{GJ}\right] \tag{22}$$

$$\bar{d}=\left[\frac{\tan\Lambda-g}{1-kg}\right]\left[\frac{qcl^3a_o\cos^2\Lambda}{EI}\right] \tag{23}$$

The solution to the eigenvalue problem defined by Eq. (18) and its associated boundary conditions is detailed in Ref. 3 for the metallic wing. The solution procedure begins by determining the homogeneous solution to Eq. (18). Next, the boundary conditions are used to define a third-order stability determinant which is a function of the parameters $\bar{a}$ and $\bar{d}$. Critical combinations of $\bar{a}$ and $\bar{d}$, denoted as $\bar{a}_D$ and $\bar{d}_D$, cause this stability determinant to be zero. The parameters $\bar{a}_D$ and $\bar{d}_D$ are those values of $\bar{a}$ and $\bar{d}$ that occur when the wing diverges.

Since the structure of the equation set describing composite wing divergence is identical to that for the metallic wing, the results published in Ref. 3 may be used, taking into account the new definition of $\bar{a}$ and $\bar{d}$ for the composite wing.

A curve of $\bar{a}_D$ vs $\bar{d}_D$ is shown in Fig. 3. The curve shown is obtained by fixing the value $\bar{a}_D$ and iteratively solving for $\bar{d}_D$. The solid curve corresponds to a stability boundary for the uniform wing. The region above the solid curve shown in Fig. 3 contains combinations of $\bar{a}$ and $\bar{d}$ that will result in a divergence condition for a swept wing, while, conversely, the region below the curve contains parameter combinations associated with a stable wing.

Also shown in Fig. 3 is a linear approximation to the stability boundary. This straight-line approximation is developed by first recognizing that, if the wing is rigid in torsion, $\bar{a}$ equals zero. A torsionally rigid swept wing diverges by bending only, in which case the exact solution for $\bar{d}_D$ is known to be (see, for instance, Ref. 12):

$$\bar{d}_D=-19/3=-6.333 \tag{24}$$

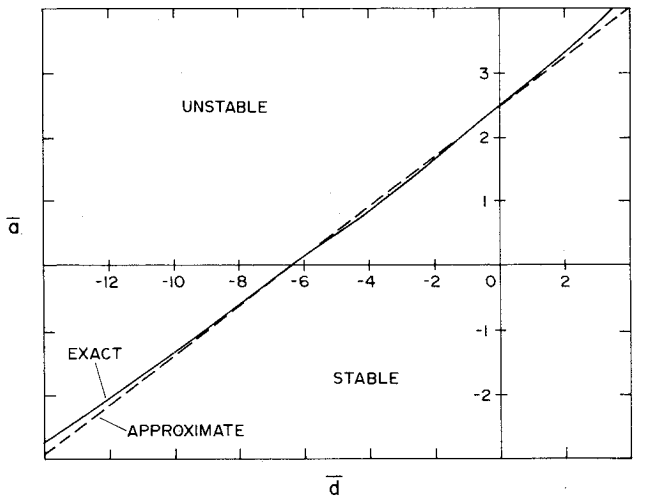

Fig. 3 The relationship between wing divergence parameters $\bar{a}$ and $\bar{d}$ for a constant chord, uniform property wing; the stability boundary relating $\bar{a}_D$ and $\bar{d}_D$ is indicated solid line (adapted from NACA TN 1680).

A different limiting condition occurs when the wing is rigid in bending ($\bar{d}=0$), but has torsional flexibility. In this case, the exact solution to the divergence problem yields

$$\bar{a}_D=\frac{\pi^2}{4} \tag{25}$$

Using the ordinate and abscissa intercepts defined by Eqs. (24) and (25), the approximate linear relationship between $\bar{a}_D$ and $\bar{d}_D$ is found to be

$$\bar{a}_D=\frac{\pi^2}{4}+\left(\frac{3\pi^2}{76}\right)\bar{d}_D \tag{26}$$

For the range of values covered in Fig. 3, the agreement between the exact solution and the approximate linear solution is excellent.

Equation (26) is useful because, by substituting the definitions for $\bar{a}$ and $\bar{d}$ into this equation, an expression for q_D, the divergence dynamic pressure, is determined to be as follows:

$$q_D=\left[\frac{2.47\,(1-kg)}{cl^3a_o\cos^2\Lambda}\right]\times\left[\frac{EI}{\dfrac{1-k\tan\Lambda}{(l/e)\,(GJ/EI)}-0.39(\tan\Lambda-g)}\right] \tag{27}$$

Equation (27) is used to obtain information about the divergence behavior of swept composite wings. First of all, it should be noted that, if q_D is a negative number, no real divergence speed occurs, since the airspeed V must be an imaginary number. For this reason, combinations of parameters that result in negative values of q_D are desirable. Attention will now turn to a discussion of the effect of groups of parameters appearing in Eq. (27) on the sign of q_D.

From strain energy considerations, it can be shown that the factor $(1-kg)$ in Eq. (27) is always positive. Thus, the denominator, containing terms dependent upon Λ and the geometric and structural characteristics of the wing, controls the sign of q_D. Furthermore, the parameter q_D becomes infinite when the following equation is satisfied:

$$\tan\Lambda_{cr}=\frac{g+2.56\,(e/l)\,(EI/GJ)}{1+2.56\,(e/l)\,g} \tag{28}$$

Values of $\tan\Lambda$ greater than that given in Eq. (28) result in negative values of q_D that, in turn, yield imaginary divergence velocities. The values of Λ determined in Eq. (28) is denoted as Λ_{cr} because, for a given structural configuration, swept wing divergence is theoretically impossible if Λ is greater than Λ_{cr}.

The parameter g is zero for a conventional metallic wing. Thus for a metallic wing operating at subsonic speeds, Λ_{cr} will be a constant greater than zero for the usual case in which the parameter e is greater than zero. This means that the metallic wing must be swept back ($\Lambda > 0$) to preclude divergence. On the other hand, with a composite material wing for which the parameter g is less than zero, the possibility exists that Λ_{cr} is less than zero. In this case, sweep angles exist, in the forward swept range, for which divergence will not occur at any flight speed. This is a significant difference between metallic and composite construction.

Two Example Cases

An example of the use of Eq. (28) to study wing divergence is provided by two different, but related, wing configurations. In the first case, all of the laminate fibers of the cover-sheets are oriented along a common direction, denoted as the angle

Table 1 Wing geometry and lamina properties

Wing aspect ratio, $AR = 6$	
Offset between aerodynamic center and reference axis, $e = 0.10c$	
Ratio of box beam depth to cover-sheet thickness 20:1.	
Lamina material properties:	
$E_1 = 32.5 \times 10^6$ psi	$G_{12} = 1.05 \times 10^6$ psi
$E_2 = 3.2 \times 10^6$ psi	$\mu_{12} = 0.36$

θ. In the second case, 10% of the fibers are fixed at an angle $\theta = 0$ deg., 25% of the fibers are oriented symmetrically at $\theta \pm$ 45 deg, 12.5% are + 45 deg, 12.5% are −45 deg, while the remaining 65% of the laminate has fibers oriented at an angle θ. Geometric and lamina material data for the wing are given in Table 1.

Figure 4 shows the relationship between the parameter $g = K/GJ$ and θ for each case. For case 1, in which 100% of the fibers can be tailored, the maximum absolute value of g is about 1.20. Note that g is an asymmetrical function (about θ = 90 deg) of θ. In case 2, where only 65% of the fibers are available for design orientation, the maximum absolute value of g is only about 0.50. In addition, the positions of the min-max values of g in the latter case lie farther away from the θ = 90 deg position than those seen for case 1.

Using Eq. (28), the relationship between Λ_{cr} and θ for the two cases can be determined. These results are shown in Fig. 5. In case 1, proper orientation of the laminate fibers can preclude wing divergence until a forward sweep angle of nearly 49 deg. This situation occurs if laminate fibers are oriented at an angle about 12 deg ahead of the swept reference axis (θ = 102 deg). For case 2, the results are less dramatic, but still impressive. When θ is about 110 deg (20 deg forward of the reference axis), the wing may still be swept forward nearly 28 deg before a real divergence speed is encountered.

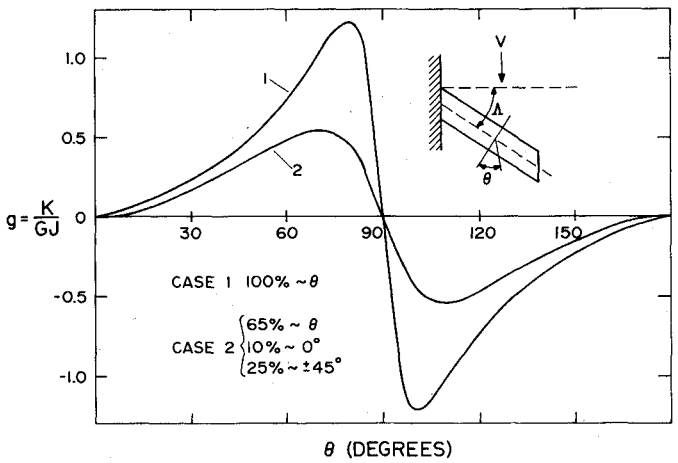

Fig. 4 Relationship between the parameter $g = K/GJ$ and fiber angle θ for two example laminates.

Turning to the effect of fiber orientation upon divergence speed, Fig. 6 plots divergence speed V_D vs the fiber angle θ for a case 1 laminate, uniform wing. These results are normalized with respect to V_{DO}, the value of V_D for the unswept wing with all the fibers oriented along $\theta = 0$. Three sweep angles are considered in Fig. 6: $\Lambda = 0$, −30, and −60 deg, corresponding to an unswept wing and two forward swept wings. In the range 0 deg $\leq \theta \leq$ 90 deg, the divergence speeds of the wing for each of the sweep angles are relatively low. However, as θ is increased beyond 90 deg and the fibers are rotated forward of the wing reference axis, the divergence speed increases rapidly. In the cases of the unswept wing and the wing with 30 deg of forward sweep, the divergence speeds become infinite for fiber angles near $\Lambda = 95$ deg. In these latter two sweep cases, there is a range of laminate fiber angles for which divergence is impossible. The range of angles in which divergence is precluded is seen to decrease with increasing forward sweep. From the results shown in Fig. 5, it is to be expected that this range, or bandwidth, approaches zero as the angle of forward sweep approaches 49 deg. Returning to Fig. 6, it is seen that, for $\Lambda = -60$ deg, a maximum divergence speed is reached when θ is approximately equal to 100 deg. For this fiber orientation, this particular forward swept wing has the same divergence speed as an unswept wing with all the fibers oriented along the reference axis ($\theta = 90$ deg).

An unusual feature of composite wing divergence is that the divergence behavior of the unswept wing is not symmetrical about $\theta = 90$ deg, even though EI and GJ are symmetrical functions about that position. For a metallic wing at zero sweep, the divergence speed is independent of the bending stiffness, since at zero sweep, bending deformation produces no lift. However, in the case of the laminated composite wing, bending deformation (caused by lift) causes torsional deformation that, in turn, leads to changes in lift. This unusual elastic coupling feature is illustrated in Fig. 6.

Linearly Tapered Wings

Next in order of complexity, after the uniform property wing, is a wing whose geometrical properties have a linear variation along the wing span. The solution to Eqs. (6) and (7) for a metallic wing ($K = 0$) whose wing chord varies linearly along the span, while the bending and torsional stiffnesses vary as the fourth power of the chord, is discussed in Ref. 3. Such a case occurs when a wing has geometrically similar

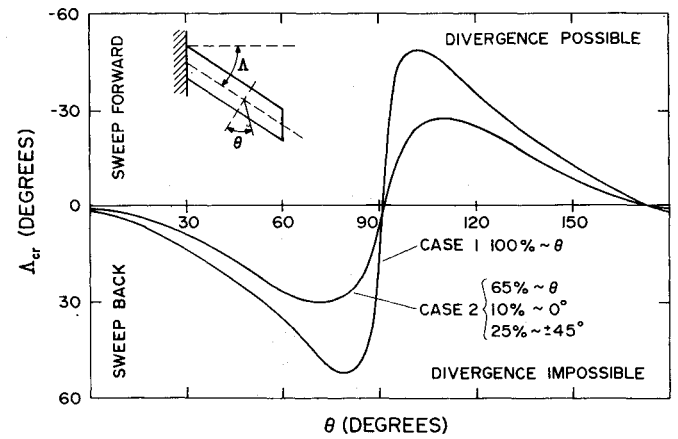

Fig. 5 Critical sweep angle Λ_{cr} vs fiber angle θ for two example laminates (uniform planform wing).

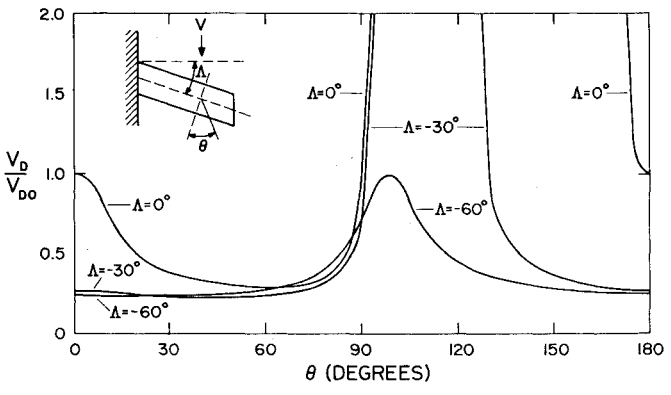

Fig. 6 Normalized divergence speed ratio V_D/V_{DO} vs fiber angle θ. All laminate fibers are oriented at angle θ (case 1), uniform planform wing.

cross sections. For a composite wing, the parameter K also varies as the fourth power of the chord for this type of wing.

With the restrictions of a linearly varying chord and geometrically similar cross-sections, expressions for problem parameters are given by the following:

$$c=fc_{\text{root}}=fc_r;\ e=fe_r;\ EI=f^4EI_r;$$

$$GJ=f^4GJ_r;\ K=f^4K_r$$

where

$(\ )_r$ = parameter value evaluated at the wing root

Transformation of Eq. (6) to the independent variable f and then nondimensionalizing, gives an equation governing bending deformation (note that $(\ )'=\mathrm{d}(\ )/\mathrm{d}f$ in the equations that follow):

$$f^3[\Gamma'''-k_r\alpha'''']+8f^2[\Gamma''-k_r\alpha'']+12f[\Gamma'-k_r\alpha']-d_T\Gamma+\frac{\mathrm{d}_T\alpha}{\tan\Lambda}=0 \tag{29}$$

where

$$\mathrm{d}_T=\frac{qc_rl^3a_o\sin\Lambda\cos\Lambda}{EI_r(1-\lambda)^3} \tag{30}$$

Similarly, the torsion equation is found from Eq. (7) to be

$$f^2[\alpha''-g_r\Gamma'']+4f[\alpha'-g_r\Gamma']+a_T]\alpha-\Gamma\tan\Lambda]=0 \tag{31}$$

where

$$a_T=\frac{qc_re_rl^2a_o\cos^2\Lambda}{GJ_r(1-\lambda)^2} \tag{32}$$

Reference 11 details how Eqs. (29) and (31) may be combined into a single equation in terms of the single variable $\alpha_e=\alpha-\Gamma\tan\Lambda$. This single governing equation reads as follows:

$$f^3\alpha_e'''+8f^2\alpha_e''+(12+\bar{a}_T)f\alpha_e'+(2\bar{a}_T-\bar{d}_T)\alpha_e=0 \tag{33}$$

where the aeroelastic parameters $\bar{a}_T$ and $\bar{d}_T$ are given by

$$\bar{a}_T=\left[\frac{1-k_r\tan\Lambda}{1-k_rg_r}\right]\left[\frac{qe_rc_rl^2a_o\cos^2\Lambda}{GJ_r(1-\lambda)^2}\right] \tag{34}$$

$$\bar{d}_T=\left[\frac{\tan\Lambda-g_r}{1-k_rg_r}\right]\left[\frac{qc_rl^3a_o\cos^2\Lambda}{EI_r(1-\lambda)^3}\right] \tag{35}$$

The boundary condition for Eq. (33) at $f=1$ ($\eta=0$) is:

$$\alpha_e(1)=0 \tag{36a}$$

At $f=\lambda$, the conditions that $M(\lambda)=0$ and $T(\lambda)=0$ give

$$\alpha_e'(\lambda)=0 \tag{36b}$$

The requirement that there be zero shear at the wing tip, when combined with Eq. (31), evaluated at $f=\lambda$, provides the following equation.

$$\lambda^2\alpha_e''(\lambda)+\bar{a}_T\alpha_e(\lambda)=0 \tag{36c}$$

Equation (33) is reduced to a linear differential equation with constant coefficients by changing the variable f to $f=e^t$. The solution to Eq. (33) subject to the given boundary conditions is presented both in Ref. 3 and Ref. 11, pp. 486-487. These details are omitted here.

Table 2 Values of F_1 and F_2 for four values of taper ratio, $\lambda=c_t/c_r$

λ	F_1	F_2
0.20	2.83	0.614
0.50	2.73	0.497
1.00	2.47	0.390
1.50	2.22	0.326

Table 3 Λ_{cr} vs for three taper ratios, $\lambda=c_t/c_r$

	Λ_{cr}, critical sweep angle, deg		
θ deg	$\lambda=0.20$	$\lambda=0.50$	$\lambda=1.0$
0	1.20	1.48	1.89
30	13.71	13.76	13.83
60	35.94	36.00	36.08
90	11.13	13.66	17.20
100	−49.08	−48.67	−48.05
120	−35.45	−35.39	−35.30
150	−13.29	−13.24	−13.16

As in the case of the uniform property wing, the solution to the equations governing divergence of a tapered wing gives critical values of $\bar{a}_T$ and $\bar{d}_T$ that occur at divergence. An approximate linear relationship again can be developed between q_D and the geometrical, structural, aerodynamic parameters in the problem. This relationship is given by the expression:

$$q_D=\left[\frac{GJ_r}{a_oc_rl^3\cos^2\Lambda}\right]\left[\frac{l}{e_r}\right]\times\left[\frac{F_1(1-k_rg_r)}{1-k_r\tan\Lambda-F_2(GJ_r/EI_r)(l/e_r)(\tan\Lambda-g_r)}\right] \tag{37}$$

The constants F_1 and F_2 are functions of the taper ratio λ and are tabulated for several values of λ in Table 2.

The effect of taper upon the divergence of swept composite wings can be seen by considering the example for which all fibers in the laminate are oriented at a common angle θ. Decreasing the taper ratio tends to decrease Λ_{cr}, although these decreases are very small, as shown in Table 3. Thus, it may be concluded that taper ratio has little influence on Λ_{cr} for this type of wing.

Figure 7 illustrates the behavior of the divergence velocity, normalized with respect to V_D at $\Lambda=0$ and $\theta=0$, as a function of θ, for $\lambda=0.20$. Comparison of Fig. 7 with Fig. 6, in which $\lambda=1.0$, shows that the tests of curves are similar, but some differences are apparent. In particular, near the fiber angle

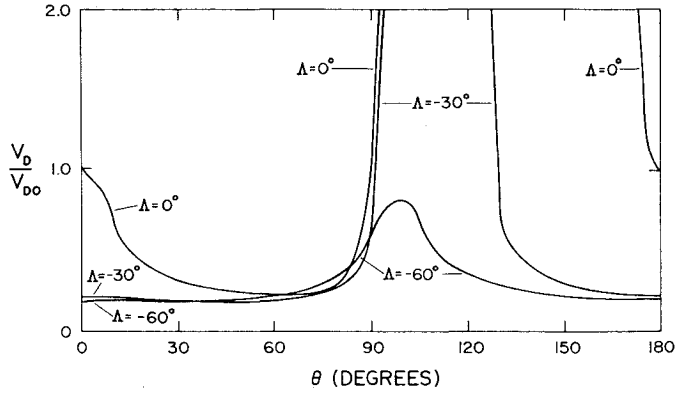

Fig. 7 Normalized divergence speed V_D/V_{DO} vs fiber angle θ. All fibers are oriented at angle θ (case 1) taper ratio $\lambda=0.20$.

$\theta = 0$ deg, the divergence velocity at $\Lambda = 0$ declines more rapidly with θ. In addition, the curve corresponding to a sweep angle $\Lambda = -60$ deg does not attain as large a maximum value when $\lambda = 0.20$ as it does when $\lambda = 1.0$. It should be noted, however, that the reference velocities are different.

Conclusions

This paper has presented a simple theory to predict the divergence behavior of moderate to high aspect ratio, laminated composite, swept wings. This theoretical development is based upon laminated beam bending theory and aerodynamic strip theory. The equations developed from this theory have been used to predict the effect of laminate construction upon wing divergence. Conclusions to be drawn from the formulas derived and the example cases presented are:

1) The elastic coupling between bending and torsion, introduced by the laminated material through the parameter k, can successfully negate the undesirable influence of forward sweep on wing divergence for large forward sweep angles.

2) The ratio K/GJ is a very important parameter to consider when designing a forward swept wing structure. This ratio should be tailored such that it has a relatively large negative value.

3) Wing taper is important to the determination of the divergence speed where such a speed actually exists. However, wing taper appears to be of little importance as a parameter influencing the design of a divergence free wing.

4) An optimal orientation for wing divergence performance appears to occur when the lamina fibers are aligned at angles of 10-15 deg forward of the swept wing box beam reference axis.

The study has shown that, from a theoretical standpoint, and unlike its metallic counterpart, the laminated composite, forward swept wing may be a feasible structural design. The formulas derived and presented in this report provide a quick, inexpensive estimation tool for further forward swept wing research.

Acknowledgment

The study presented in this paper was supported by AFOSR Grant 77-3423 with funding provided by the Defense Advanced Research Projects Agency (DARPA).

References

[1] Holzbaur, S., "Sweptforward Wings," *Interavia*, Vol. V, No. 7, 1950, pp. 380-382.

[2] Kramer, E. H. and Smilg, B., "The Effect of Sweepforward on the Critical Flutter Speed of Wings," Engineering Div. Memo. TSEAC5-4595-2-6, Army Air Forces Air Material Command, Wright Field, Ohio, April 1946.

[3] Diederich, F. W. and Budiansky, B., "Divergence of Swept Wings," NACA TN 1680, Aug. 1948.

[4] Jones, L. S., *U.S. Bombers, B-1-B-70*, Aero Publishers, Los Angeles, 1962.

[5] *Jane's All the World's Aircraft*, McGraw-Hill, N.Y., 1970-71, pp. 105-106.

[6] Knight, M. and Noyes, R. W., "Span Load Distribution as a Factor in Stability in Roll," NACA Rept. 393, 1931.

[7] Krone, N. J., Jr., "Divergence Elimination with Advanced Composites," AIAA Paper 75-1009, 1975.

[8] Housner, J. M. and Stein, M., "Flutter Analysis of Swept-Wing Subsonic Aircraft with Parameter Studies of Composite Wings," NASA TN D-7539, Sept. 1974.

[9] Austin, F., Hadcock, R., Hutchings, D., Sharp, D., Tang, S., and Waters, C., "Aeroelastic Tailoring of Advanced Composite Lifting Surfaces in Preliminary Design," *Proceedings of AIAA/ASME/SAE 17th Structures, Structural Dynamics, and Materials Conference*, 1976, pp. 69-79.

[10] Jones, R. M., *Mechanics of Composite Materials*, McGraw-Hill, N.Y., 1975, pp. 45-59.

[11] Weisshaar, T. A., "Aeroelastic Stability and Performance Characteristics of Aircraft with Advanced Composite Sweptforward Wing Structures." Air Force Flight Dynamics Laboratory, AFFDL-TR-78-116, Sept. 1978.

[12] Bisplinghoff, R. L., Ashley, H., and Halfman, R. L., *Aeroelasticity*, Addison-Wesley, Reading, Mass., 1956.